Rose-Hulman Institute of Technology

2007 ASME East Coast HPV Competition

Single Rider Entry

Team Members

Tommy Roberts
Zach Goff
Danny Sing
Molly Nelis
Chris Wlezien
Michael Wieck
Jeffery Van Treuren

Blake Lin
Luisa Fairfax
Nathan Wendt
Pooja Saxena
Christina Davis
Justin Gerretse

Table of Contents

Abstract

During the East Coast HPV challenge in 2006, the Rose-Hulman *Hautian Hazard* placed 8th overall. For 2007, we have refined, reinvented, and reborn our short-wheel base recumbent bicycle to be faster, safer, and sexier. The result of our efforts is the Rose-Hulman 2007 single-rider entry, the *R5*.

Figure 1: The 2007 Rose-Hulman *R5*

The R5 is the natural evolution of our previous entry. Its distinctive aerodynamic shape and red paint scream "drive me" while the short wheel base provides the vehicle with the sporty feel it implies. A clear PETG plastic canopy allows for maximum visibility, while the carbon fiber and Kevlar composite fairing protects the rider inside. A steel frame anchors the structure, and a revised front wheel drive system propels the R5 to blistering new speeds.

The R5 is not only an evolution in design, but a representation of the growth of our team. It will be the first entry for Rose-Hulman into multiple competitions. The first of which was the Nissan one hour record challenge, April 6th-8th 2007. By competing in early competitions, our team has more hours to practice and refine our design to be the fastest and safest vehicle possible. Our team's knowledge has grown as well. As a result, extensive use of Computer Aided Design programs, Cosmos finite element analysis, and FloWorks computational fluid dynamics software has increased the effectiveness of the vehicle design.

Rose-Hulman's previous entry, *The Hautian Hazard* had a top speed of 38 mph. With the *R5*, our team has set its sights on a top speed of 50 mph. We believe through extensive research, analysis, and real-world testing, our vehicle has the capability of attaining these goals, while simultaneously being among the safest vehicles in field.

Design Specifications

The two basic goals of our design are to develop the safest vehicle possible and create a vehicle capable of breaking 50 mph. In order to develop criteria and set goals for our rolling and air resistance values, we created a Matlab program to graph theoretical vehicle performance at various power levels. In order to make use of this program, a theoretical human power output was needed. The figure below represents data taken by NASA to gauge human performance.

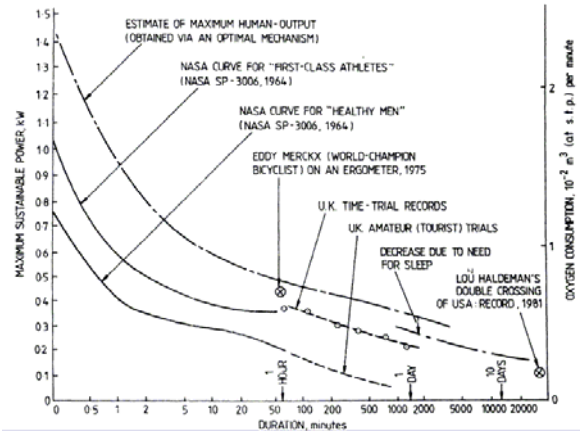

Figure 2: Estimate Curves for Human Power Output [9]

Using figure 2 as a reference, the theoretical maximum output for a healthy male is 500 watts. This is the number that we have aimed for in our simulation. Using a standard rolling resistance coefficient (.005), we changed the CdA value until the curve crossed the 500 Watt line at 50 mph. Figure 3 illustrates the results.

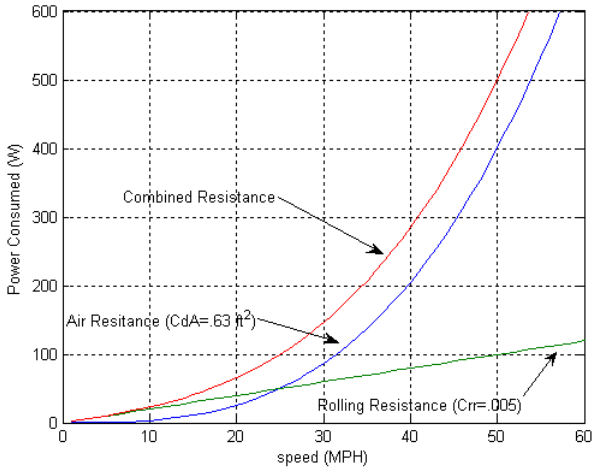

Figure 3: Power Curve for Ideal HPV entry

From Figure 3 and the Matlab program, we were able to determine a number of design goals in order to reach our 50 mph speed. From Figure 2 it was decided that the rolling resistance coefficient is a small aspect of the equation. Since air resistance takes over, more efforts must be focused on drag. Using this data, we were then able to quantify our goals and develop a table to illustrate them.

Table 1: Design Goals

Team Goal	50 mph Sprint Speed
Aerodynamic Goal	$C_d \cdot A \leq .63\ ft^2$
Rolling Resistance	Tires with $C_{rr} \leq .005$
Safety	25 ft. turn radius Brake from 15 to 0 mph in $\leq 20\ ft.$ Additional Redundant Braking System Travel 100 ft. in straight line Chrome-moly steel tube roll cage of 1.5" OD and wall thickness of .049 Safety harness (seatbelt) ≥ 3 points Rider Protection from sliding

Design

Frame

The frame was designed to place the rider in a position that would minimize frontal area as well as provide a shape to fit a body of revolution for a laminar flow fairing. For more information on the theory behind laminar flow, see section fairing design. A highly reclined position suits these criteria best. Once a general position of the rider was set, actual frame setups were considered.

Before brainstorming frame geometries, the frame material was first determined to balance the various properties of strength, weight, stiffness, fabrication time, vibration damping, material cost and aerodynamic effects. The materials considered were aluminum 6061-T6, Hexcel's EH04 epoxy composite system coupled with IM4 carbon weave, normalized 4130 chromolly steel, titanium 6AL-4V and Red Oak. The choice was determined using a decision matrix as documented in Appendix A, and it was found that tubular steel was the best frame material to use.

A top down design methodology was used to first locate the important components as shown in figure 4. Later in the analysis section, several frame geometries that connect these components are considered. To aid in fitting a human rider, M.V.Ficarra's configurable human model iMike was used. By designing to the largest rider, the smaller riders are guaranteed to fit inside the fairing.

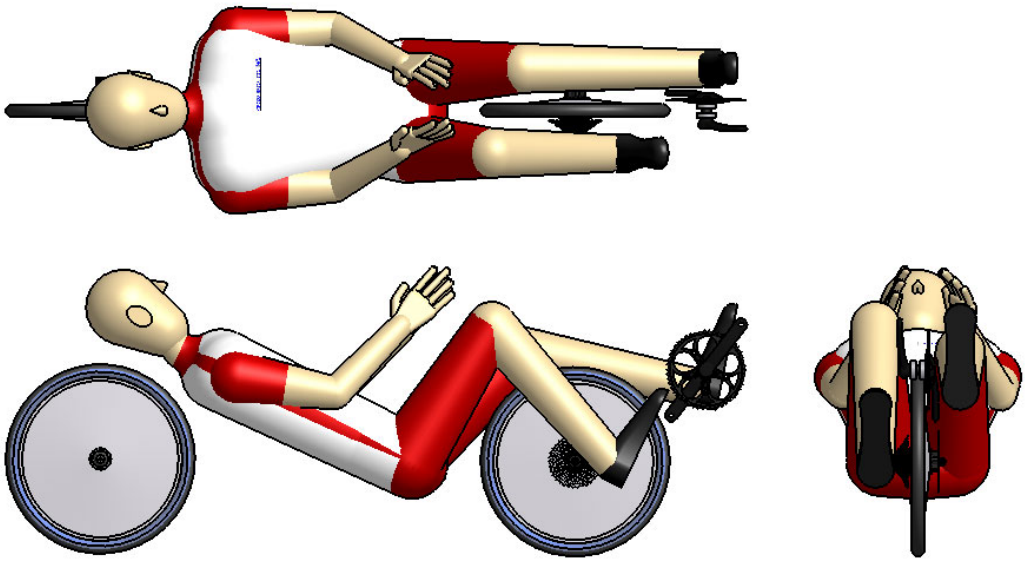

Figure 4: Rider Layout

Drive Train

The drive train is one of the most important aspects of reliability on a bicycle. A poorly designed drive train will cause excessive losses and will decrease the reliability of a bike. A well designed drive train will make the bicycle both more efficient and more user friendly.

Traditional bicycles use a rear wheel drive system. The advantages of a traditional rear wheel drive system are things that most riders take for granted. Rear wheel drive systems do not torque steer with the pedal stroke and they leave plenty of space for the gearing system. The cassette and derailleur can be placed at the rear wheel well out of the way of the rider's feet. As downsides they have longer drive lines and require more chain tensioners. On a low racer type recumbent it is more complicated to get the chain from the cranks to the rear wheel than on a traditional bicycle due to the distance and lack of a straight path. Additionally the longer chain often feels unnervingly slack to the rider. Front wheel drive systems on the other hand have their share of downsides. Front wheel drive systems often have chain rub on the front wheel on sharp turns. They also must be designed in a much more compact fashion than a rear drive system to fit within the front of a small faired recumbent. The cassette can be placed at the

hub or at an intermediate gear system near the head tube. A third option is an internally geared hub. The main advantages of internally geared hubs are space and simplicity. There are no issues with finding a place for a derailleur as with traditional front drive systems. Due to this the chain line is much more compact and easier to fit no matter which wheel is powered. Because it is a single speed chain system up to the hub the chain drive is simpler and more reliable. As the chain does not need to change length with gear changes less chain tensioners are needed. Additionally, internally geared hubs can be shifted when the rider is not pedaling. While they are slightly less efficient than a standard cassette system the main drawback of internally geared hubs is the cost. A good internally geared hub will cost at least twice that of comparable traditional components. While space considerations are less of an issue for front wheel drive systems, internally geared hubs still feature some torque steer on front wheel drive and still have awkward chain lines in rear wheel drive systems. Overall, the best balance of cost and effectiveness is the front wheel cassette drive set-up.

At the base of the drive train are the cranks. Other than placement and wheel interference which are controlled by the frame design, the main two variables with crank assemblies are length and q-factor. Crank length is measured as the distance from the axis of the bottom bracket spindle to the axis of the pedal. Q-factor, or tread, is "The lateral distance between the pedal attachment points on a crankset."[4] By decreasing those measurements you can shrink the size of the front of the fairing. The power cost of shorter crank arms is decreased torque. However, when done in moderation the increased cadence allowed in a recumbent position by the decreased crank arm length compensates for the torque loss. The minimum effective crank arm length is controlled by the ability of the rider to "spin" at a high cadence rather than "mash" at a low cadence. For our bicycle we found that 155 mm crank arms were a good balance and also fit within our fairing. The cost of a narrow tread is frame flex and frame clearance. Frame flex from a narrow bottom bracket can be compensated for with a thicker bottom bracket shell. Clearance issues then become the limiting factor. A tread of 107mm was chosen as it was as narrow as possible without causing clearance issues.

Because the tread was decreased mainly by shortening the bottom bracket spindle, a narrow bottom bracket shell had to be made. The bottom bracket was made to be adjustable so that the bicycle could be tuned to different riders for the sprint event. The shaft was keyed to prevent the crank assembly from rotating about the main tube.

A mid drive was chosen because it allowed the derailleur to be out of the way of the rider's heel. This is a good location as there was already an intermediate shaft in that location. With 20 inch wheels it is necessary to use a greater gain ratio than on standard bicycles with 700c size wheels. This is overcome by using a large chain ring on the crank set or an intermediate shaft. While the large chain ring method removes the need for a step up shaft, the shaft is still needed to redirect the chain in front wheel drive systems. Additionally large front chain rings, while popular on world record setting recumbents, have problems with front wheel interference on even large radius turns. Using an intermediate shaft also allows the crank to drive on the left side of the frame. This is because the intermediate shaft can serve as a pass through point to transfer the driving forces to the right side of the frame and down to the wheel. By keeping the two separate chains on opposite sides of the wheel the chains will not contact each other when turning.

Due to the 20 inch tire used on the drive wheel and the limitations requiring a standard gearing to be used on the front chain ring a step up gear was needed. In order to achieve our goal speed of 50 mph with a desired cadence of 110 rpm we determined that a 22:13 step was needed:

$$\frac{104 rev_{crank}}{1 min}\left|\frac{60 min}{1 hour}\right|\frac{53 teeth}{1 rev_{crank}}\left|\frac{22 teeth_{intermediate}}{11 teeth_{intermediate}}\right|\frac{1 rev_{wheel}}{13 teeth_{wheel}}\left|\frac{20 \cdot \pi inches}{1 rev_{wheel}}\right|\frac{1 ft}{12 in}\left|\frac{1 mile}{5280 ft}\right| = 50.46 \frac{miles}{hour} \quad \text{EQ. 1}$$

A cadence of 110 rpm would allow a top speed of 53.37mph.

Damping System

Laminar flow can be prematurely tripped into turbulent flow through vibrations induced by road noise. To help dampen these vibrations a simple head tube suspension was built based on a design by Warren Beachamp. The suspension compresses a polyurethane cylinder which, along with the friction of the support bushings, is self damping. Flanged bronze bushings allow rotational and linear movement and a threadless handlebar stem clamps

the assembly together. A thin disk of elastomer at the top of the headshock limits top out. This; in addition to the relatively large amount of frame flex from a single beam frame design and wide tires, helps smooth road vibrations thus maintaining laminar flow.

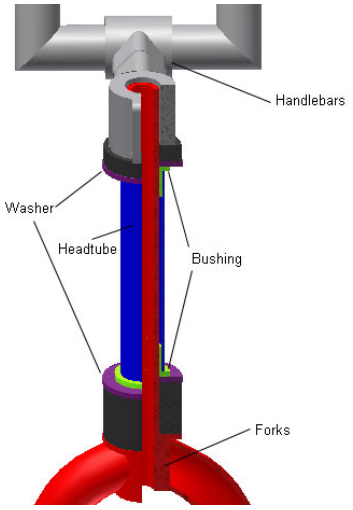

Figure 5: Head Tube Suspension

Stability and Control

The ability to handle a human powered vehicle easily is important when multiple riders must be trained to ride unfamiliar bicycle configurations in races where multiple vehicles are present. To properly design the front end steering geometry, Bill Patterson's optimal high speed trail equation (EQ_) is used. This equation is derived in Lords of the Chainring to determine the appropriate trail based on locations of center of mass with respect to the ground and rear wheel, and seatback angle. By using the belly button as an approximation of the bike's center of gravity (Beauchamp W. 1998) and estimating a total vehicle weight of 200lbs, 4 in of trail was found to give good high-speed handling characteristics. Choosing a small amount of conventional positive offset, a headtube angle could then be determined to give 4 in of trail.

$$T = K5 \cdot \frac{B}{M}\left(\frac{1}{Kx^2} + \frac{1}{h^2}\right) \qquad \text{EQ. 2}$$

T: Trail
K5: steering feel, a value of "jet fighter" or 0.5 is used to reduce trail and thus fork flop
B: horizontal distance of center of gravity to rear axle
M: mass
Kx: radius of gyration, related to seatback angle and can be looked up in a table
h: center of gravity height from ground

Braking

A combination of a front disk brake with a rear caliper brake is utilized as the braking system. From experience last year, it was concluded that front and rear caliper brakes did not have adequate stopping power for recumbents at the higher speeds seen in racing. Our vehicle from last year had issues with the brake pads overheating and smoking with several different types of brake pads in emergency stop tests. Given that brake pads decompose when heated, and that the high rim temperatures associated with overheating rim brakes can cause tire blowouts, it was decided that the main brake would not be rim based. Knowing that this year's vehicle would be faster it was decided that a more robust brake system would be needed. Cantilever and linear pull brakes have more stopping power but are also rim based and therefore can have the same problem of overheating the rims. While drum brakes were considered it was decided that disk brakes would be easier to integrate into the bicycle due to hub availability, cost, and brake cable pull distance. While the front disk brake should provide sufficient cooling to sustain frequent braking for turns on the course a backup was needed. While it does not have sufficient braking and cooling power

for frequent use caliper brakes are capable of stopping the vehicle in an emergency situation such as the failure of the disk brake. Additionally the rear wheel bears much less weight than the front making it more susceptible to skidding and losing control under the greater braking loads which can be applied via a disk brake. For these reasons the rear is equipped with a caliper brake with carbon/aluminum rim compatible brake pads. These have been chosen because they have higher maximum operating temperatures and do not decompose in the event that they are overheated.

Ergonomics

To obtain maximum power from the rider we had to design the bike with the angle of the seat with respect to the ground in mind. If the seat was at to high of an angle we would increase our cross sectional area and our CDA value. This would increase the amount of power the rider would have to put out and be less efficient. On the other hand if the seat angle is too low the rider will not be able to see as well and he/she would be able to at a higher angle. Furthermore, if the angle is low the rider cannot push against the seat and cannot deliver power. With all of this in mind we decided on a seat angle of 23˚. This angle is optimal because; it allows for the rider to be able to press up against the seat as they pedal, it gives the rider a good view of the track, and it keeps the cross sectional area of the bike down.

In order to allow a range of different users of the bike to see properly out of the canopy, the bike needed to be adjustable. To best due this we decided to make the seat an adjustable component. Our first generation seat (top-left figure 6) was just a quick mock up to prove the concept was feasible. Our second generation (top-right figure 6) seat was a more contouring carbon fiber design in order to be more comfortable for the rider. This was to be adjustable by a lifting it by a clap that raised and lowered around a drop down bar. This design had to pivot at the bottom of the seat and this was not acceptable because it raised the whole seat up to high to still keep the cross sectional area down. We decided on our third design (bottom fig. 6) because the seat was mounted stationary and the adjustability came from the foam padding we would put on it to raise the rider. For shorter riders we would use the 2″ pads and for taller riders we would use the 1/2″ pads.

Figure 6: Evolution of Seat Design. Top Left - First Seat Top Right - Donated Carbon Fiber Seat Bottom - Final Wood and Foam Seat

On a well designed road or mountain bike the handlebars are shaped such that the hands are in their natural position. This can be confirmed by having the rider release their grip on the handlebars and placing their hands in the position that they find most natural for their wrist. The exception to this is time trial bars where the aerodynamic benefits of a less comfortable hand position are justified. The same was done with the controls on our bicycle. The rider was placed within the bicycle and asked to put their hands in the most natural position. After some brief calculations to

ensure that that position would allow the handlebars to fit within the fairing at the maximum turn angle the handlebars were fabricated to those dimensions. The brakes and shifter were then added in the position which required the least amount of hand movement from the original hand position.

To allow riders of different heights to reach the pedals we needed to make our bottom bracket adjustable. In order to do this we created our bottom bracket out of aluminum solid and cut a slot into it where it slides onto the frame (from figure 7) to make it clamp down when the bolts on the top of the bracket are tightened. These bolts can be loosened and the bracket can be brought in and out depending on the height of the individual rider.

Figure 7

In order to alleviate potential neck strain and do to the rider holding their head up while riding, we added a neck rest. The decision was for a neck rest not a head rest. This is to keep the drivers vision clear due to the fact that if it was a headrest it would literally shake the drivers head and not allow him to see straight.

Fairing

The lowest drag shape about an object would ideally have no flow separation, and maintain laminar flow for as long as possible before going turbulent. Turbulent flow has a skin friction drag of approximately 10 times higher than laminar flow. In order to maintain laminar flow as long as possible, a favorable pressure gradient is created by constantly sloping the sides outward. The real trick is to do this for as long as possible while bringing the fairing back together not too quickly to cause flow separation. The lowest CdA of Fairing 4 which is 12 ft shows how a long tail helps lower aerodynamic drag, unfortunately its large size makes it impractical to ride and transport. Other than fairing 4, the best shape was fairing 3. The final design of fairing 5 was accomplished by shaping and streamlining fairing 3 to look streamlined. This follows the design philosophy "if it looks fast then it will go fast," by George Georgiev, the builder of the worlds fastest human powered vehicles.

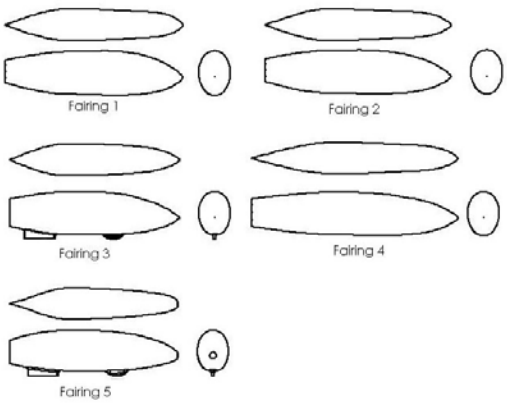

Figure 8: Evolution of fairing designs

Table 2: Fairing CdA values

Fairing Design	CdA Value	Speed (m/.s)	Force (newtons)	Mesh Refinement (Accuracy)
Fairing 1	0.185	20.1	4.25	3
Fairing 2	0.391	20.1	9.06	3
Fairing 3	0.164	20.1	3.77	3
Fairing 3	0.574	20.1	13.2	7
Fairing 4	0.143	20.1	3.3	3
Fairing 5	0.56525	20.1	13	7

Pitting Procedures

An auxiliary consideration beyond the function and safety of the bike is quick pitting during the endurance event. The capability to quickly reconfigure the bike for different riders, and make getting into and out of the bike was considered in the design.

The Styrofoam seat inserts are the most important component in interchangeability. For the male riders a ½ inch thick pad is attached to the seat with industrial strength Velcro. For the female riders an identical 2 inch pad is used so it is easier to reach the pedals. Changing the pads takes only seconds and requires no tools.

Several features were included to ensure that the bike is simple to enter and exit. The large bubble leaves ample space to enter, and requires no squeezing or twisting. The bubble is attached with tape. In order to exit the rider pushes the bubble up with their hands and the tape seal breaks with very little effort. Small pegs were welded on the fork near the axle to help the rider position in the seat. These pegs are often found on BMX bikes, and give the rider something to brace against besides the fairing.

Before the competition a landing gear wheel will be installed to help with staying upright as the rider is stopping. Since the rider's feet cannot touch the ground a small third wheel helps with balance so a pit crew member doesn't need to steady the bike whenever the rider wants to stop or start or enter.

Analysis

Frame strength/stiffness

Several frame geometries are considered to balance characteristics of strength, weight, ridgidity, ease of rider changeability, and simplicity of manufacture. Figure 1 shows the evolution of different geometries as placed in a CosmosWorks simulation showing stress and deflection. The combined rider and vehicle weight was estimated at 200 lbs. Using a factor of safety of 3 to account for additional stresses from crashes and road bumps, a total loading of 600 lbs was applied along the seat and back beams. Proper loading constraints are essential for accurate finite element analysis results. A pin joint on the front wheel axle and a pin in slot joint in the rear allows the proper deflection characteristics to occur.

Frame 4 was the first frame proposal and utilized extremely thin walled tubing in a vertical double beam arrangement that proved exceptionally light and strong. It would also allow multiple attachment points for the fairing. Unfortunately the thin walled chromolly tubing sections were not readily available and so the design became heavier than single-beam variants. This in addition to complexity of manufacture and increased difficulty in swapping riders nixed the design.

Frame 1 is the immediate response to the problems associated with Frame 4. It retained the previous front end triangulation while using the thicker cross-sectional tubing in a single beam design, however it showed signs of buckling under load.

Frame 2 used a larger 2 in diameter tubing in the buckling region; however, the stiffness of the triangulated front concentrated stresses at the bottom of the frame. Frame 3 further simplified this triangulated region and reduced the stresses. Stress concentrations would be dealt with by using large-filleted welds with plenty of filler metal. Initially frame stiffness was a concern, but the flexure can provide additional shock absorption thus easing the harshness of the ride and helping to maintain laminar flow.

The welding process used to join the tubular sections was Tungsten Inert Gas (TIG) for the high quality welds it produced. Following conventional race car frame welding techniques, the filler metal of choice was American Welding Society (AWS) ER70S-2 which is a low carbon steel filler that reduces the chance of brittle martensite forming in the weld puddle since further heat treatment after welding was not an option.

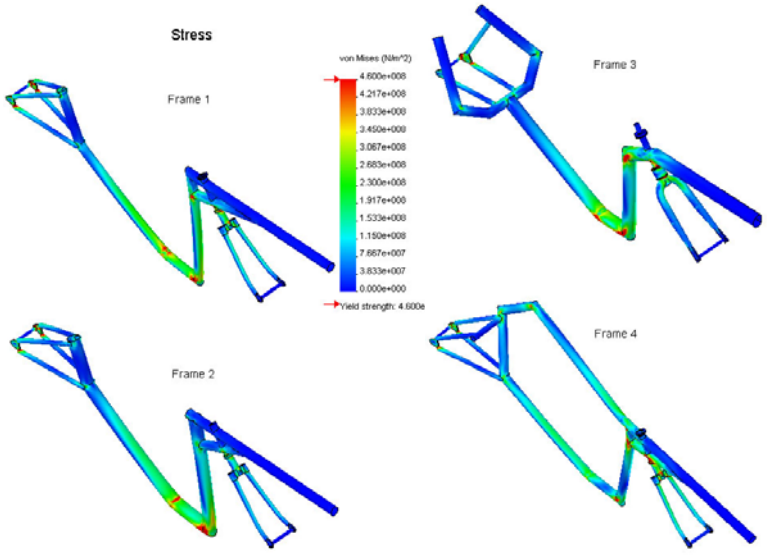

Figure 9a: Bike Frame Analysis

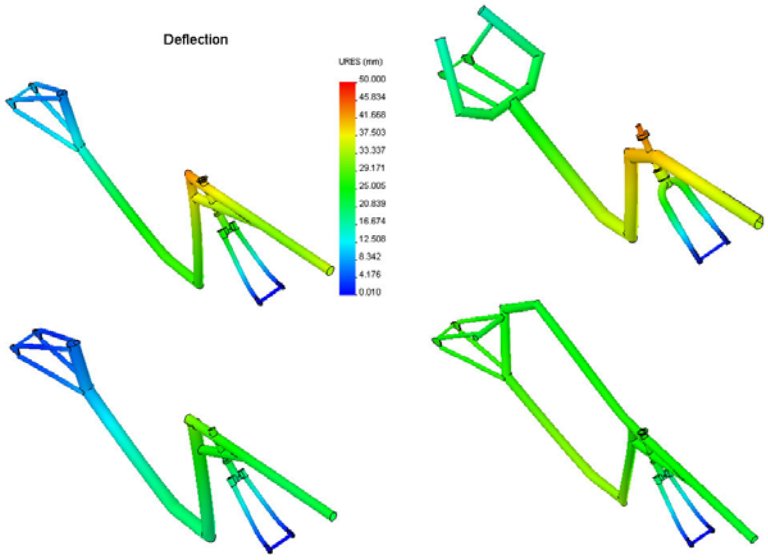

Figure 9b: Bike Frame Analysis

Suspension

After fabricating the suspension using bronze bushings as outlined earlier in the design section, it was found that sitting in the bike caused the suspension to lock up and also create a large amount of resistance in turning the wheel. Further research into the head tube design showed that a variant had been successfully implemented on a recumbent bicycle with a nearly vertical head tube. As our design called for a large head tube angle to increase trail, additional side loading forces were applied to the bushings and friction forces prevented the fork tube from freely sliding inside the bushings.

Figure 10: Nearly Vertical Head Tube Suspension

In order to see if this design was salvageable by using lower resistance bushing material such as Delrin, a static model to calculate the frictional forces retarding sliding motion was developed and is explained in Appendix C. Using a steel-sintered bronze friction coefficient of 0.16, the force retarding sliding motion when the frame is loaded to 200lbs turns out to be 177 lbs which is greater than the axial force pressing the forks into the head tube (125 lbs). This explains why the head tube locks up when the frame is loaded. If the friction coefficient is reduced to 0.05 which is for heavily loaded delrin and steel, then the frictional forces are reduced to 53 lbs and the suspension can then slide inside the bushings, although with a very high damping coefficient that limits its effectiveness in damping small vibrations from road noise.

Aerodynamics

Using Floworks, each of the possible fairing designs was sent through a computational fluid dynamic simulation. The results were then scrutinized and used to continually develop further Cad models. The figure below details the pressure gradients and flowlines for the two most successful models. Initially, we ran the models with a small mesh, but later, the best fairing were run with a better mesh and a floor to simulate ground effect on the vehicle. Floworks was able to calculate force exerted on the body, and using the aerodynamic force equation, we converted these numbers into CdA values.

$$Force = \tfrac{1}{2}\rho C_d A V^2 \qquad \text{EQ. 2}$$

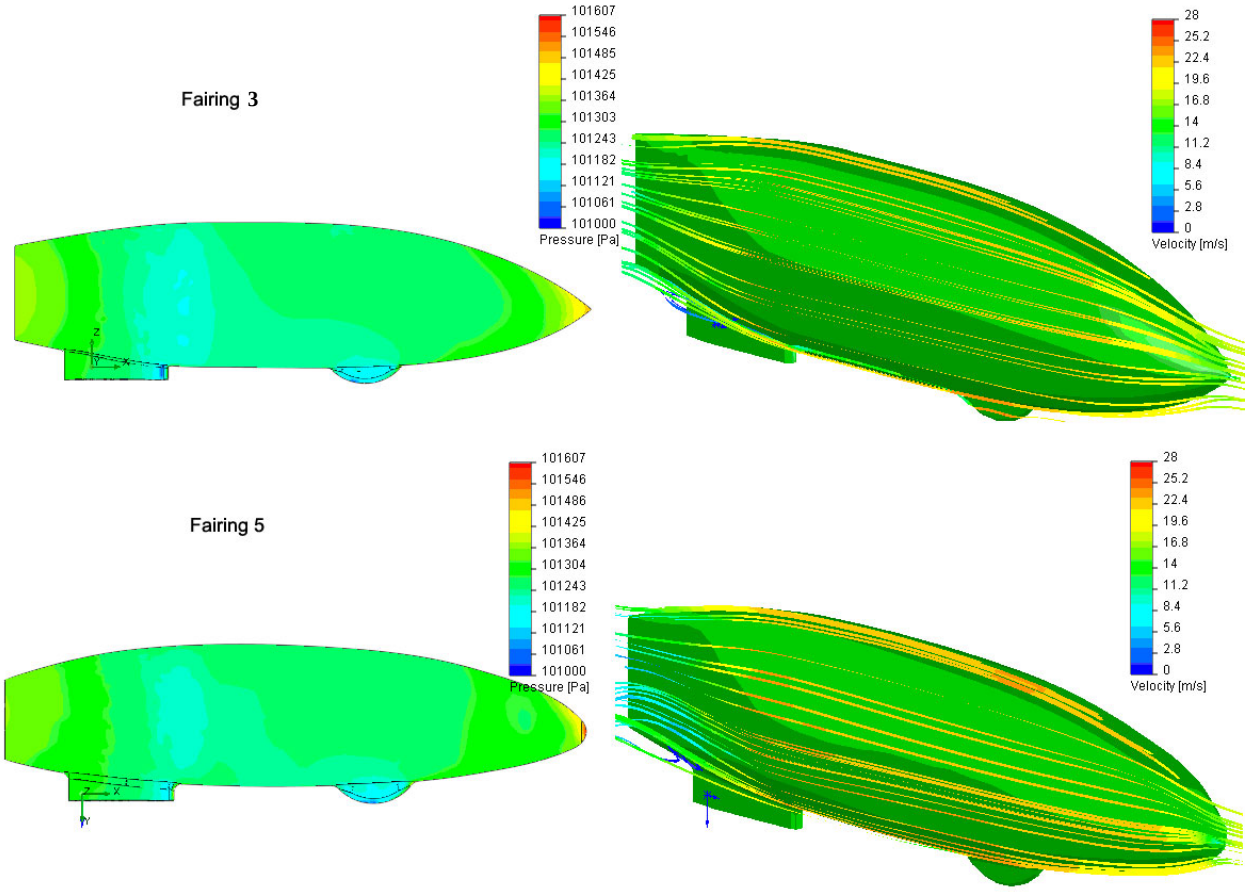

Figure 11: Floworks Examples

Testing

Coefficient of Rolling Resistance (CRR)

An important factor in the overall speed of the vehicle is rolling resistance. From figure 5 it is shown that aero drag only overcomes rolling resistance at a speed of 25 mph, and it is a large component of overall drag. Efforts to lower rolling resistance involve using wide-rimmed tires with a high aspect ratio such as the Michelin Ecorun. In order to calculate the CRR, a test was conducted using a tricycle.

Figure 12: Rolling Resistance Testing Tricycle

A person rode on the tricycle which was placed on a wooden incline 0.3048 m high and 1.553 m long. After leaving the incline, the surface was a linoleum tile floor. By equating the kinetic energy of the vehicle leaving the ramp to the energy lost due to rolling resistance, the CRR can be determined

Figure 13: Tricycle, Incline and Tile Floor Track

Figure 14: Testing the Coefficient of Rolling Resistance

Each test was conducted in the same location and with the same rider. Because this was a comparison test, the slight tilt of the floor was ignored. Aerodynamic drag forces were also considered negligible due to the low velocities involved (less than 1.0 m sec^{-1}). Additionally, the ramp's CRR was ignored. It was assumed that the tricycle left the ramp at approximately the same speed. However, if the tricycle wheels had a higher CRR and left the ramp at a slower speed, then it would travel a shorter distance. Thus, a higher CRR and lower velocity would be reflected in the relative calculation. The equation for CRR is as follows.

$$CRR = \frac{F_r}{F_N} \qquad \text{EQ 3}$$

This is calculated only for the front wheel. Thus, the normal force is equal to the weight of the front wheel including the rider. The rolling resistance force is calculated as follows:

$$E_{kinetic} = \frac{1}{2} m_{total} v^2 \qquad \text{EQ 4}$$

The velocity, v, was measured by putting magnetic bike sensors on the wheel. In order to increase the sensitivity at a low speed, four magnets were placed on the wheel. The velocity measured was:

$$\frac{4\frac{\text{m}}{\text{s}}}{4} = 1\frac{\text{m}}{\text{s}} \qquad \text{EQ 5}$$

$$F_r = \frac{E_{kinetic}}{d} \qquad \text{EQ 6}$$

Test A uses Michelin Ecorun tires on all three wheels. Test B uses Avocet Fasgrip Carbon 12 tires on all three wheels. Test C uses a Primo Comet front tire (from last year's vehicle) and Avocet Fasgrip tires on the rear wheels.

Table 3: Crr Data Results

Test	Distance Rolled (m)	CRR
Test A @ 60 psi	39.78	0.002209
Test A @50 psi	33.48	0.002624
Test A@ 40 psi	32.01	0.002745
Test B @ 110 psi	28.41	0.003092
Test C @ 110 psi	26.71	0.003290
Test B @ 80 psi	25.64	0.003426
Test B @ 50 psi	20.02	0.004388

As shown above, the best coefficient of rolling resistance is from the Test A Michelin Ecorun tires at a pressure of 60 psi. The best CRR is 0.002209 with an error of 16.32%. Additionally, a trend can be seen. Higher pressures provide lower CRRs. Calculations and error propagations are included in Appendix B.

Turning Radius

The rules state that the vehicle must be able to turn within a 25́ radius. To achieve this we had to create a sufficient front wheel cutout in the fairing for the wheel to turn inside of. At the same time we could not make the cutout any larger than it would have to be to turn because then we would be creating needless losses in aerodynamics.

The specifications on our handle bars are also dependent on our turning radius. If handles were to far away from where they meet up with the head tube the bike would not be able to achieve the 25́ turning radius because the bars could not rotate far enough in the fairing. On the other hand if the bars were to close to where they meet up with the head tube the riders knees would run into the handles while they were pedaling. We chose a length of 130 mm to accommodate for both of these problems.

Fairing materials - Testing samples:

In an effort to figure out the optimal order of layers for the composite fairing four samples of ½ inch by 1 ½ inch layers of fiberglass, carbon fiber and Kevlar. The samples were made with the same cup of epoxy, and left for a day and a half to harden. The samples were put into a vice and bent with a pair of pliers until failure. The samples were

inspected to see which ones had significant splinters. Severe splintering of the fairing could injure the rider in the event of a crash, so minimizing that risk was important for rider safety.

Sample 1 was from outside to inside fiberglass, Kevlar, carbon fiber.
Sample 2 was from outside to inside fiberglass, carbon fiber, Kevlar.
Sample 3 was from outside to inside fiberglass, Kevlar, carbon fiber, Kevlar.
Sample 4 was from outside to inside fiberglass, Kevlar, carbon fiber, fiberglass.

Figure 15: The top-left picture is of sample 1. Note the long shard at the break. This failure mode disqualified this arrangement. The top-right picture is of sample 2. The surface is fuzzy after the break with several blunt shards. The bottom-left picture is of sample 3. There is little fuzz, and more shards than sample 2. The bottom-right picture is of sample 4. There are two or three blunt shards at the break.

The final decision on fairing material was to use the combination of sample 2, while laying down the extra outer layer of Kevlar where the fairing was likely to slide on the ground in the event of a crash. The effectiveness of this patch is shown in the picture below.

Figure 16: The picture on the left is of the fairing before it was painted. The yellow patch is the extra Kevlar. The picture on the right is of the fairing after a crash on asphalt. The scratches on the paint line up with where the patch was placed.

Nissan One Hour Record Challenge

The Nissan One Hour Record Challenge is a race put on by the Human Powered Vehicle Association at the Nissan test track in Casa Grande, Arizona. From the previous years vehicle, we knew one of our problems was lack of testing time. In order to overcome this obstacle, we decided that a real-world test scenario would be best. We

chose the Nissan Challenge because it is held before this design report is due. Also, this event was host to twenty human powered vehicles, from new prototypes, to the veteran world record holding Varna Diablo 2 & 3. An opportunity to view and learn from these professionals seemed like an amazing chance for our team.

There were two events held at the Nissan Challenge. Single person one hour attempts and 200 meter speed attempts like those in the HPVC. Through running in both these events, we have developed a table for the problems we encountered at the event, and how we will fix them.

Figure 17: 14 of the 20 hpvs assembled for a picture at Nissan

Table 4: Problems encountered at Nissan

Problem Encountered	Reasoning For Problem	Solution
Torque Steer of bike (more notable at higher cadence)	Since the chainline does not come down through the steering axes, it causes excessive pull on the hub of the wheel.	Add a chain guide to route the tension side of the chain along the steering axis.
Chain Derailments	Cross-Chaining, bumps in the road, and sudden stops in pedaling caused chain derailments in both 1 hour attempts.	A chaingaurd on the front chainring is being added.
Fairing Mount	Velcro initially failed for front mount. Mounts were also to high, causing nose to be high.	New Fairing mounts are being developed. These composite and metals mounts will be more secure, and won't be so adjustable as to have nose height problems.
Need for Landing Gear	Riders falling from failing catching attempts.	Add Landing Gear to enable vehicle to stop without assistance.
Width	Compared to all the HPVs at the competition, the *R5* is over 8 inches to wide.	The *R5* fairing could be slimmed, drastically reducing frontal area. This is unlikely to occur.
Front Suspension	The front wheel drive system increased chain tension as you are pedaling. This increase in tension is absorbed by the rubber in the suspension, robbing power from the rider.	Unfortunately, the font suspension will be removed to prevent this power loss.

During the Nissan event, only our 20 inch avocet tires were used. We did not switch tires to Michelin Ecoruns because of our limited quantity. We decided it was best to use them only at our main event, the East Coast HPVC. Below is a figure for the projected curve of necessary power to travel at different speeds in the R5. Our sprint speed was only measured at 40.2 mph. This translates to 275 watts. This reflects problems in torque steer (shown in above table) as well as rider health.

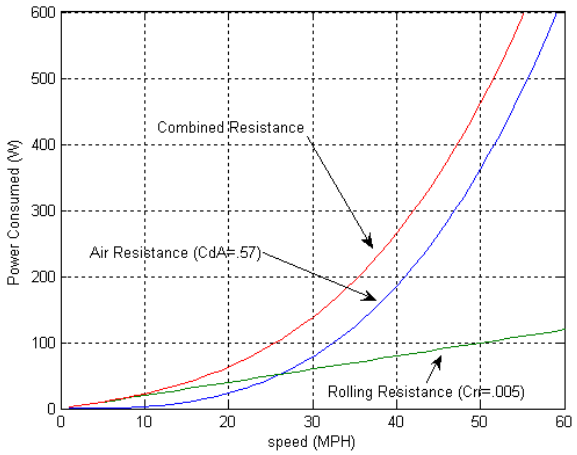

Figure 18: Power Curve for R5 at Nissan Event

Using the Michelin Ecoruns the power curve we expect at ASME is shown below.

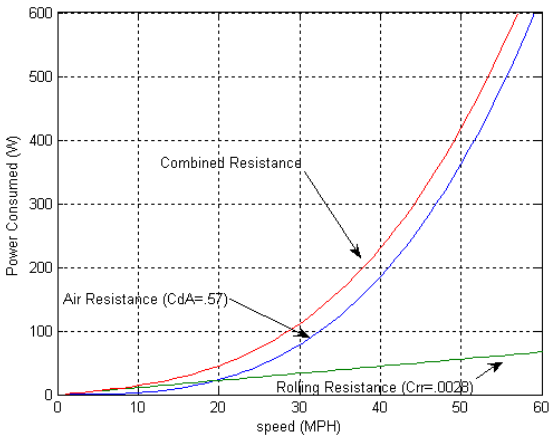

Figure 19: Projected Power Curve for R5 at ASME HPVC

As shown in Figure 19 , with Ecorun tires and at 425 watts sustained, we could break our goal of reaching 50 mph in a sprint event. This means our rider must be in good health, and trained for the event.

Safety

Frame Material

In order to provide enough strength and to give a little flex in our frame, we decided to go with 2″ chrome-molybdenum steel tubing with a 0.049″ wall thickness. Further development of frame strength is found in the Analysis section.

Seat Belt

In the event of a crash or collision we had to make sure the rider was properly secured in the bike and inside of the roll cage. We decided to use a 4 point seat belt in order to secure the rider down adequately; where as a standard lap belt may allow the rider to slide up the seat with their head then protruding from the roll cage. We decided on rivets to attach the seat belt to the bike. This method of attachment proved very effective when used on our bike from last year's completion and so we felt no need for any changes.

Side Protection

We decided to make our shell out of a composite material that is not uniform over the body in order to provide the different aspects of protection we need in different areas of the bike. From the inside out the fairing is made of a layer of Kevlar that covers the entire fairing except for the canopy. The next is a layer of carbon fiber that that again covers the entire body minus the canopy. The next layer is only a partial layer in order to provide extra protection in the areas we would most likely skid on if we were to crash during a race. There is an extra layer of Kevlar spanning a large portion of both sides and a small portion covering the back wheel fairing (see figure 20). Kevlar was the obvious choice for reinforcing the area that the bike is likely to skid on because of it high resistance to wear. Over all of this we laid a layer of fiberglass to give us a surface to sand and paint. This combination of layers does not only allow for the bike to skid across the ground without wearing through the fairing, which protects the rider inside, but it also protects the rider from any blunt force that may strike the bike in the form of another vehicle. If this kind of collision were to occur the rigidity and tensile strength of the composite walls of the fairing would keep the shell from deforming and thus the entire bike would be pushed by the impact without breaking the walls. To protect the bike even further some stiffening ribs were built on the inside of the fairing

Figure 20: Kevlar sections

Roll Cage

The rules dictate that we must have a roll cage that would protect the rider in the event of the bike flipping over in an accident. To ensure rider safety we decided to have two roll cages so that every point between them would be protected not just the riders head and upper body. The head roll cage is made of 1.5″ chrome-molybdenum steel tubing with a 0.049″ wall thickness as specified in the rules, and it extends above the head in a halo like fashion. The foot or lower roll cage extends beyond the front of the pedal box and supports the fairing as well as protects the

rider. With the two combined roll cages there is no way the rider can be hurt from skidding during a crash because no matter the orientation or direction of the slide the rider is safe because he/she is always under the line drawn between the two.

Field of View

In order to maximize our field of view we decided to build an oversized canopy that covered the top of the fairing that is directly in front of the riders head all the way to his/her peripherals on both sides (from figure 21). With this large viewing area it is easy to avoid accidents and navigate well.

Figure 21: Clear Canopy

Other hazards

Accident protection from the most obvious sources (skidding on the ground and colliding with other vehicles) is easy to avoid with proper safety features built into the early design, but some dangers are not apparent until the bike is ridden. One thing we noticed is the cassette is in a dangerous position if we were in fact to get into an accident. It is right next to the rider's knees and if the bike were to fall over there is no telling what could happen from its sharp teeth. To prevent any damage to our bodies for the cassette, we constructed a guard made of carbon fiber and Kevlar (from figure 22). This guard not only keeps the driver from hurting himself in the event of an accident, but it also keeps anything from happening if the rider accidentally hits their knee into while pedaling.

Figure 22 : Kevlar Cassette protection

Another issue we ran into after we built the bike way the fact that the chain was rubbing on the front tire when we turned right. To solve this problem we built a chain fender. It keeps the chain from ever touching the wheel during the turns and therefore it removes any possibility of the tire popping due to chain rub.

Another danger that is often overlooked is communication. If something were to happen to the driver of the vehicle or something were to happen outside of the driver's knowledge that could cause harm to him/her then there would need to be communication between the vehicles or the team and the vehicle. The major problem with this is that the faired vehicle is very noisy and almost impossible to hear anything in. Our solution is a device know as a temple transducer. It relays sound from our onboard radio through the driver's temples so they can hear despite the noise around them. This allows the driver to always be clear on what is being communicated to them so they can respond quickly to whatever may happen.

Appendix A: Frame Material Decision Matrix

Various factors that contribute to frame performance for a streamlined recumbent bicycle were identified. Quantifiable data was found for each category if at all possible. The data is then normalized on a scale from 0 to 1, where a 1 represents the best value, and 0 the worst. The normalized values are then multiplied by an importance factor that relates the importance of any category to our specific design goals and constraints. For example, cost was a large factor for us so it received an importance of 3, whereas weight is not so much an issue in racing streamliners so density received an importance factor of 1. The values for the properties of each material are then summed, and the highest material score is the best for the application.

Strength and Weight

Having lightweight frame allows a bike to accelerate faster, lowers rolling resistance and increases handling. A material that has good strength and low density will produce the lightest frame, so the two should be considered together.

Stiffness

A stiff frame prevents flexing under load. This is important because a frame that flexes under pedaling forces robs the rider of a small fraction of power. A more important reason for streamliners is that a flexing frame can deform the fairing, which can disrupt the aerodynamic shape and create excessive drag. The overall stiffness of a frame is largely determined by its geometry rather than modulus of elasticity. For example, steel has a much larger stiffness than aluminum, however the necessary cross section of a steel member is smaller than that of aluminum, and so the stiffness of an aluminum frame can approach that of steel.

Fabrication Time

Due to time constraints in getting the vehicle to competition, the time to fabricate is very important and received an importance factor of 3. This category assumes a well trained fabricator skilled in working with the material of choice.

Vibration Damping

A material's ability to dampen small vibrations such as road noise is important in preventing rider fatigue and in maintaining laminar flow over the fairing, which can prematurely transition to turbulent due to significant oscillations in the 50-500Hz range. However, the effects of frame vibration damping are difficult to quantify and so this category received a low importance factor.

Aerodynamics

The human powered vehicle is already assumed to have a streamlined fairing around the frame. As such, flow over each material is not considered. This category accounts for each materials unique ability to keep the fairing in an ideal aerodynamic shape. Materials with low strength to volume characteristics would increase the frontal area of the bike, thus becoming undesirable. Materials that can be easily contoured into complex shapes provide flexibility that lead to decreased frontal area.

Cost

The project has a budget, thus cost is a significant factor. An ideal frame would be low cost, as more money could be budgeted toward the drive mechanism and aerodynamic fairing.

Table 5: Frame Material Decision Matrix

Material	Tensile Strength (Mpa)	Normalized Strength	Density lb/in^3	Normalized Density	Stiffness (Gpa)
Importance Factor	2.0000		1.0000		2.0000
Al 6061-T6	276.0000	0.2435	0.0975	0.7070	68.9000
Steel 4130	460.0000	0.4092	0.2840	0.0000	205.0000
Ti 6Al-4V	880.0000	0.7873	0.1600	0.4701	113.8000
Carbon Fiber	2227.0000	2.0000	0.0610	0.8453	124.8000
Wood, Red Oak	5.5000	0.0000	0.0202	1.0000	12.5000

Material	Normalized Stiffness	Aero	Normalized Aero	Cost of Materials (USD)	Normalized Cost
Importance Factor		3.0000		2.0000	
Al 6061-T6	0.5860	0.3000	0.9000	53.6000	1.8835
Steel 4130	2.0000	0.6000	1.8000	42.7000	1.9600
Ti 6Al-4V	1.0525	0.5000	1.5000	209.2800	0.7910
Carbon Fiber	1.1668	1.0000	3.0000	322.0000	0.0000
Wood, Red Oak	0.0000	0.0000	0.0000	37.0000	2.0000

Material	Fabrication Time (hours)	Normalized Time	Vibration Damping	Normalized Vibration	Overall Score
Importance Factor	3.0000		1.0000		
Al 6061-T6	9.0000	3.0000	0.2000	0.0000	7.3200
Steel 4130	9.0000	3.0000	0.6000	0.5000	9.6692
Ti 6Al-4V	11.0000	2.0000	0.7000	0.6250	7.2258
Carbon Fiber	15.0000	0.0000	1.0000	1.0000	8.0121
Wood, Red Oak	10.0000	2.5000	1.0000	1.0000	6.5000

Appendix B: CRR Sample Calculations

The following documents an example calculation for Test A @ 60 psi in determining the tire CRR and measurement error.

Table 6: Measurements

Value	Measurement
Mass (m)	101.9 kg
Mass, front wheel ($m_{front\ wheel}$)	59.09 kg
Displacement	39.78 m

$$E_{Kinetic} = \frac{1}{2}mv^2 \qquad \text{EQ 7}$$

$$F_r = \frac{E_{kinetic}}{d} = \frac{\frac{1}{2}\times 101.9\times 1^2 \text{ Joules}}{39.78 \text{ m}} = 1.281 \text{ Newtons} \qquad \text{EQ 8}$$

$$F_N = m_{frontwheel} \times g = 59.09 \times 9.81 = 579.7 \text{ Newtons} \qquad \text{EQ 9}$$

$$CRR = \frac{F_r}{F_N} = \frac{1.281 \text{ Newtons}}{579.7 \text{ Newtons}} = 0.002209 \qquad \text{EQ 10}$$

Rolling Resistance Error Propagation

$$CRR = \frac{F_r}{F_N} = \frac{\frac{1}{2}\times m \times v^2}{d \times m_{frontwheel} \times g} \qquad \text{EQ 11}$$

Table 7: Uncertainty in Measurements, CRR

Item	Random	Systematic	Total
Mass, total (kg)	0.05000	0.05000	0.07071
Mass, front (kg)	0.05000	2.000	2.001
Distance (m)	0.0005000	0.001000	0.001118
Velocity (m/s)	0.125	0.005	0.1251

$$Total = \sqrt{random^2 + systematic^2} \qquad \text{EQ 12}$$

$$Total_{mass} = \sqrt{0.05^2 + 0.05^2} = 0.070 \qquad \text{EQ 13}$$

Table 8: Percent Error

Item	Uncertainty	Measurement	% Uncertainty
Mass, total	0.07071 kg	101.9 kg	0.00069
Mass, front	2.001 kg	19.09 kg	0.10
Distance	0.001118 m	33.48 m	3.3×10^{-5}
Velocity (m/s)	0.1251 m/s	1 m/s	0.13

$$\left(\frac{\delta crr}{crr}\right)^2 = \left(\frac{\delta m}{m}\right)^2 + \left(\frac{\delta m_{front}}{m_{front}}\right)^2 + \left(\frac{\delta d}{d}\right)^2 + \left(\frac{\delta v}{v}\right)^2 \qquad \text{EQ 14}$$

$$\frac{\delta crr}{crr} = \sqrt{0.0006939^2 + 0.1048^2 + (3.339\times 10^{-5})^2 + 0.1251^2} = 0.1632 = 16.32\% \qquad \text{EQ 15}$$

Appendix C- Friction forces in Suspension

By using a static model of the head tube suspension, the frictional forces retarding sliding motion of the steer tube on the bushings can be found. Summing forces in the vertical direction as well as the moments about the rear wheel axle, the weight on the front wheel *Ffw* can be found.

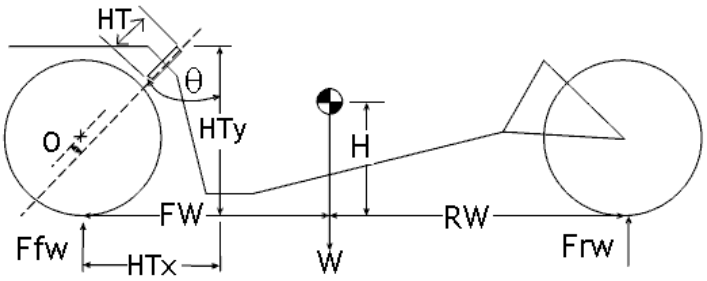

Figure 23: Force Diagram for Head tube Suspension Analysis

$$0 = Ffw + Frw - W \qquad \text{EQ 16}$$

$$0 = Frw \times (FW + RW) - W \times FW \qquad \text{EQ 17}$$

Looking closer at the front wheel and head tube in Figure _, equations of forces in the X and Y directions, as well as a sum of moments about the wheel center. Gathering dimensions from the CAD model of the bike allows solving for the normal forces *a* and *b*, between the bushings and fork, as well as the force *c* pressing the forks into the suspension elastomer.

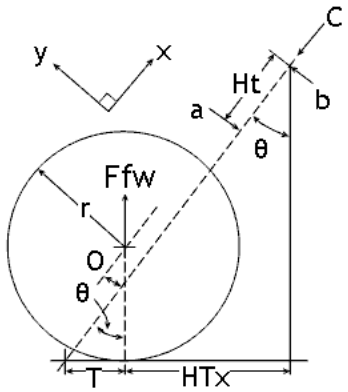

Figure 24: Detail Force Diagram of Front Wheel Suspension

$$0 = -c + Ffw\cos(\theta) \qquad \text{EQ 18}$$

$$0 = b - a + Ffw\sin(\theta) \qquad \text{EQ 19}$$

$$0 = b\frac{HTx}{\sin(\theta)} - a\left(\frac{HTx}{\sin(\theta)} - HT\sin(\theta)\right) \qquad \text{EQ 20}$$

Solving for static frictional forces F_f between the steer tube and bushings allows a comparison to the force *c* pushing the forks into the elastomer. When *Ff* < *c* then the steer tube is capable of sliding on its bushings. A very small *Ff* is ideal for a smooth, low hysteresis suspension where the elastomer bears most of the bike weight.

$$F_f = \mu_s(a + b) \qquad \text{EQ 21}$$

Appendix D- Costs

Table _: Parts List

Description	Qty	Unit Cost	Total	Purchased from	Item #
Frame materials	1	$ 237.60	$ 237.60	Aircraft Spruce	n/a
Seats	1	$ 110.00	$ 110.00	Power On Cycling	n/a
Cranks	1	$ 59.50	$ 59.50	QBP dealer catalog	CR4764
Bottom Brackets	1	$ 22.94	$ 22.94	QBP dealer catalog	CR4802
Front (non-drive)	1	$ 36.00	$ 36.00	QBP dealer catalog	HU8414
hubs (drive)	1	$ 34.25	$ 34.25	QBP dealer catalog	HU6602
spokes/nipples	72	$ 0.08	$ 5.76	Hed Cycling Products	n/a
rims	2	$ 27.16	$ 54.32	QBP dealer catalog	RM7555
Cassettes	1	$ 19.68	$ 19.68	QBP dealer catalog	FW8421
Cassettes	1	$ 49.00	$ 49.00	QBP dealer catalog	FW8380
Derailleurs	1	$ 54.24	$ 54.24	QBP dealer catalog	RD6601
Chain	2	$ 7.68	$ 15.36	QBP dealer catalog	CH4091
Shift Cables	2	$ 0.95	$ 1.90	QBP dealer catalog	CA5000
Brake Cables	2	$ 1.54	$ 3.08	QBP dealer catalog	CA4211
Brake cable housing	1	$ 5.40	$ 5.40	QBP dealer catalog	CA4250
Gear cable housing	1	$ 9.00	$ 9.00	QBP dealer catalog	CA4335
Disc brakes	1	$ 52.80	$ 52.80	QBP dealer catalog	BR5997
4 point seatbelts	1	$ 30.00	$ 30.00	Ebay	n/a
Tires	2	$ 60.00	$ 120.00	Rose Supermileage	
Tubes	4	$ 1.51	$ 6.04	QBP dealer catalog	TU4518
shifters (pair)	1	$ 43.50	$ 43.50	QBP dealer catalog	RD0704
Freebody	4	$ 13.30	$ 53.20	QBP dealer catalog	FW8909
Brake Lever (pair)	1	$ 12.50	$ 12.50	QBP dealer catalog	BR7323
Fairing	1	$ 800.00	$ 800.00	US Composites	n/a
Hardware	1	$ 600.00	$ 600.00	McMaster Carr	n/a
Total			**$2,436.07**		

Table _: Overall Expenditures

Employees	
Welder	$2,500
Machinist	$2,500
Workers	$8,320
Engineer	$3,750
Capital Costs	
Building Rent	$3,000
Utilities	$1,000
Equipment	$1,000
Advertising	$1,500
Shipping	$300
Plug Construction	$1,450
Cost per Month	$25,320
Additional cost per unit	$2,532
Total cost per unit	$4,968.07

Works Cited

[1] Patterson, W. B., 2004, *The Lords of the Chainring* Santa Maria

[2] Hexcel Corporation, 2005, "HexPly EH04," Product Data, http://www.hexcel.com/NR/rdonlyres/7C2AC220-0513-4620-897B-9A52813A41C5/0/HexPly_EH04_us.pdf

[3] Automation Creations, Inc, 2007, "MatWeb," Material Property Data, http://www.matweb.com/index.asp?ckck=1

[4] Brown, S., 2007, "Frame Material for the Touring Cyclist," Material analysis, http://www.matweb.com/index.asp?ckck=1

[5] Ficarra, M. V., 2003, "iMike," humanoid CAD model, http://www.xanadu.cz/download.asp?file=iMike

[6] Beauchamp, W., "Headshock V2," Suspension information, http://www.wisil.recumbents.com/wisil/headshock/headshock.htm

[7] Beauchamp, W., "Steering Trail Calculators," Steering information, http://www.wisil.recumbents.com/wisil/trail.asp

[8] Beauchamp, W., "Headshock V2," Suspension information, http://www.wisil.recumbents.com/wisil/headshock/headshock.htm

[9] Owers, D, J., 1985 "Development of a Human-Powered Racing Hydrofoil," Human Power, **3,** "3" pp. 13